

## Biosynthesis

How to cite: *Angew. Chem. Int. Ed.* **2022**, *61*, e202203264

International Edition: doi.org/10.1002/anie.202203264

German Edition: doi.org/10.1002/ange.202203264

# Sequential Allylic Alcohol Formation by a Multifunctional Cytochrome P450 Monooxygenase with Rare Redox Partners

Hak Joong Kim, Keishi Ishida, Mie Ishida-Ito, and Christian Hertweck\*

In memory of Klaus Hafner (1927–2021)

**Abstract:** Caryoynencin is a toxic and antifungal fatty acid derivative produced by a number of plant-pathogenic and insect-protective bacteria (*Trinickia caryophylli* and *Burkholderia* spp.). In addition to the reactive tetrayne unit, the presence of an allylic alcohol moiety is critical for antimicrobial activities. By a combination of mutational analyses, heterologous expression and in vitro reconstitution experiments we show that the cytochrome P450 monooxygenase CayG catalyzes the complex transformation of a saturated carbon backbone into an allylic alcohol. Unexpectedly, CayG employs a ferritin-like protein (CayK) or a rubredoxin (CayL) component for electron transport. A desaturation-hydroxylation sequence was deduced from a time-course study and in vitro biotransformations with pathway intermediates, substrate analogues, protegencin congeners from *Pseudomonas protegens* Pf-5, and synthetic derivatives. This unusual multifunctional oxygenase may inspire future biocatalytic applications.

## Introduction

Cytochrome P450 monooxygenases (CYPs) are a large superfamily of heme-dependent enzymes endowed with the capacity to oxidize a broad range of compounds. In all domains of life, CYPs not only play essential roles in detoxification processes but also in the biosynthesis of highly diverse natural products.<sup>[1]</sup> From a chemical point of view, CYPs are fascinatingly versatile biocatalysts as they func-

tionize non-activated carbon atoms with high precision, typically with outstanding regio- and stereoselectivity. Moreover, CYPs introduce a range of oxygenation patterns into their substrates by means of C- and N-hydroxylations, dehydrogenation of alcohols and aldehydes, desaturations, and epoxidations.<sup>[2]</sup> Intriguingly, some CYPs have evolved that mediate multiple oxygenations, such as oxygenations at two different sites, and various sequential modifications that are still difficult or impossible to emulate with chemical reagents and catalysts.<sup>[3]</sup>

We have discovered a gene (*cayG*) tentatively coding for a multifunctional CYP in a gene cluster (*cay*) for the biosynthesis of a rare bacterial polyynone named caryoynencin (**1**, Figure 1).<sup>[4]</sup> Initially isolated from the carnation wilt pathogen *Trinickia caryophylli* (formerly assigned to the genera *Pseudomonas*, *Burkholderia*, and *Paraburkholderia*),<sup>[5]</sup> this toxic fatty acid metabolite is also produced by *Burkholderia gladioli* strains, including a mushroom pathogen<sup>[6]</sup> and a beetle symbiont that protects the insect eggs from entomopathogenic fungi.<sup>[7]</sup> Although the exact mode of action of caryoynencin is not yet known, synthetic studies on structural analogues revealed that, in addition to the terminal alkyne, the presence of the secondary alcohol is critical for antimicrobial activity.<sup>[8]</sup> Preliminary mutational analyses by single-crossover insertional disruption indicated that *cayG* plays an important role in caryoynencin biosynthesis. The resulting mutant is incapable of forming **1** but instead produces, as the major metabolite, a congener (**2**) lacking the allylic alcohol moiety.<sup>[4]</sup> Interestingly, the same compound (named protegencin, aka protegenin) is also produced by *Pseudomonas protegens*, which bears a gene cluster homologous to the *cay* gene locus but lacks a CYP gene.<sup>[9]</sup>

While these findings indicated that CayG plays a role in caryoynencin biosynthesis, the biosynthetic route to the pharmacophoric allylic alcohol remained enigmatic. Here we show that CayG catalyzes the complex transformation of the saturated carbon backbone. We shed light on the biochemical basis of this biotransformation, elucidate the mechanism sequential allylic alcohol formation, and present CayG as a novel multifunctional monooxygenase using two unusual redox partners.

[\*] Dr. H. J. Kim, Dr. K. Ishida, Dr. M. Ishida-Ito, Prof. Dr. C. Hertweck  
 Dept. of Biomolecular Chemistry, Leibniz Institute for Natural  
 Product Research and Infection Biology, Hans Knöll Institute (HKI)  
 Beutenbergstr. 11a, 07745 Jena (Germany)  
 E-mail: christian.hertweck@leibniz-hki.de

Prof. Dr. C. Hertweck  
 Faculty of Biological Sciences, Friedrich Schiller University Jena  
 07743 Jena (Germany)

Part of the "Special Collection in Memory of Klaus Hafner".

© 2022 The Authors. Angewandte Chemie International Edition published by Wiley-VCH GmbH. This is an open access article under the terms of the Creative Commons Attribution Non-Commercial License, which permits use, distribution and reproduction in any medium, provided the original work is properly cited and is not used for commercial purposes.

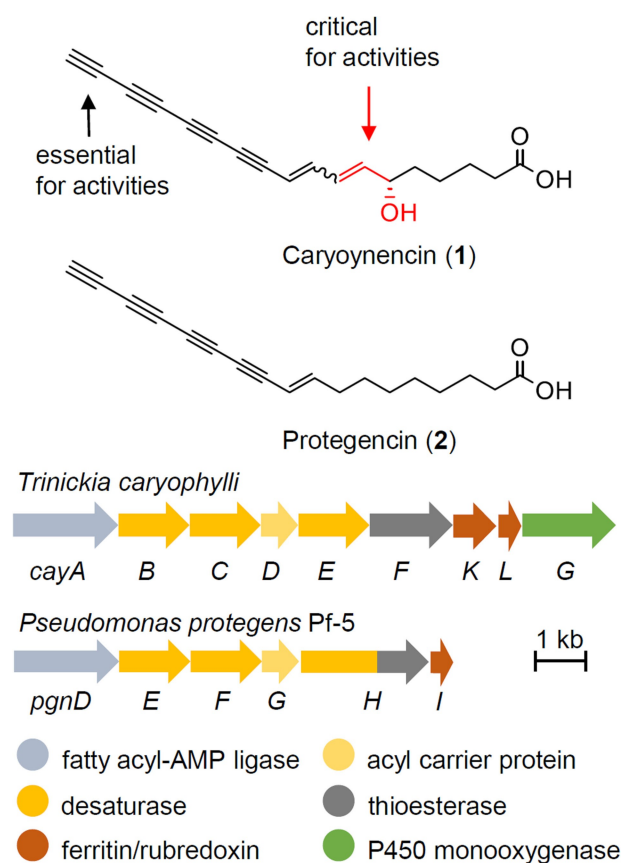


**Figure 1.** Structures of the bacterial polyynes caryoyne (1) and protegenin (2), and architectures of the corresponding biosynthesis gene clusters.

## Results and Discussion

To systematically investigate the enzymatic function of CayG and to clarify whether this biocatalyst would promote a multistep-transformation involved in allylic alcohol formation, we approached this task from two different angles: a) by targeted gene deletion in the caryoyne producer, and b) by engineering the protegenin-producing pseudomonad into a recombinant strain making caryoyne.

The initial functional assessment of *cayG* was based on a single crossover, which may lead to polar effects.<sup>[4]</sup> Thus, for the targeted gene deletion (approach a), we employed an improved method in which we replaced the target gene with an apramycin resistance cassette by double-crossover knock-in<sup>[9b]</sup> (Figure S1). As expected, the resulting *cayG* null mutant strain produces 2 in lieu of 1 (Figure 2A, trace b).

To test whether co-expression of *cayG* confers to *P. protegens* the ability to convert the polyne 2 into 1 (approach b) we cloned *cayG*, ligated it into an expression vector (pJB861) downstream of the inducible Pm promoter,<sup>[10]</sup> transformed *P. protegens* and induced gene expression by addition of *m*-toluic acid. Monitoring the metabolic profile of the transformant by HPLC-DAD and HRMS, however, did not show any difference to the control bearing the empty vector only (Figure 2B, traces a–b). Thus,

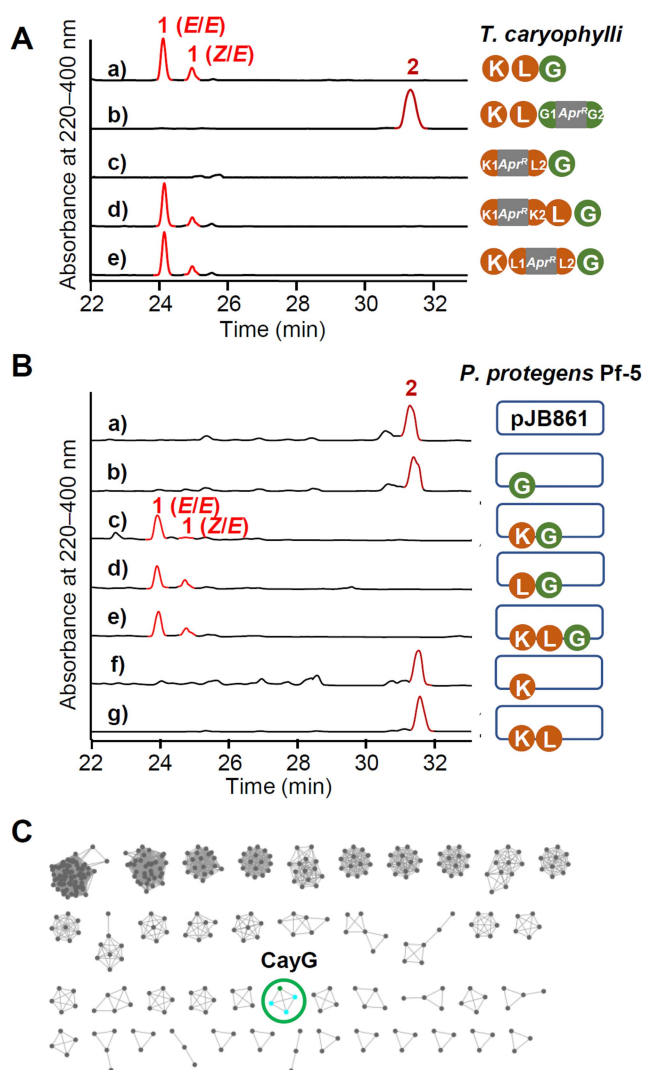


**Figure 2.** Mutational analysis of the oxygenase components, and heterologous reconstitution of caryoyne biosynthesis. A) HPLC-DAD profiles of culture extracts of *T. caryophylli* wild type (a) and mutants lacking individual genes or gene sets (b)–(e). B) HPLC-DAD profiles of culture extracts of *P. protegens* Pf-5 transformants a) with empty pJB861 vector (control), and b)–f) expressing individual genes or gene sets. C) Sequence similarity network (SSN) of CayG (green). CayG specific node is circled in green. Other CayG homologs of *Burkholderia* species shown as cyan dots.

we concluded that CayG is essential but likely not sufficient for the transformation of 2 into 1.

In order to identify the missing components, we scrutinized the *cay* and *pgn* gene loci with particular focus on the differing gene region downstream the thioesterase gene. We noted that the *cay* gene cluster bears two previously overlooked genes (*cayK*, *cayL*) for a ferritin-like protein<sup>[11]</sup> (Figure S2) and a rubredoxin<sup>[12]</sup> (Figure S3), respectively, whereas only one gene (*pgnI*) for a rubredoxin is present in the *pgn* gene cluster. We investigated the roles of *cayK* and *cayL* by deleting either the gene pair or each gene individually. Surprisingly, polyne production is fully abolished in the absence of both *cayK* and *cayL* (Figure 2A,

trace c), but unimpaired in mutants lacking either *cayK* or *cayL* (Figure 2A, traces d–e). This result indicates that at least CayK or CayL are required as redox partners of the desaturases, CayB, CayC, and CayE. It appears that the absence of one part of the electron transfer system, either CayK or CayL, may be tolerated (because of a redundant function) or complemented by the two rubredoxins encoded elsewhere in the genome (Figure S3).

To investigate the impact of CayK and CayL on the CayG-mediated biotransformation *in vivo*, we heterologously expressed the ferritin-like protein/rubredoxin and CYP genes in various combinations (*cayKLG*, *cayKG*, *cayLG*, *cayKL*, *cayK*) in *P. protegens*. HPLC-DAD analysis of the culture extracts revealed that the co-expression of *cayKLG*, *cayKG* or *cayLG* yields **1** (as a mixture of its *E,E*- and *Z,E*-isomers) as in the wild-type producer (Figure 2A, trace a and Figure 2B, traces c–e). These results unequivocally show that CayG has to be minimally paired with either CayK or CayL in order to achieve the conversion of **2** into **1**.

CayL is likely required for electron transfer to the desaturases involved in polyene formation, because *cayL* orthologues are highly conserved in all bacterial polyene biosynthetic gene clusters (Figure S4), whereas *cayK* is only present in the *cay* gene cluster.<sup>[9a,13]</sup> Genome neighborhood analysis<sup>[14]</sup> of CayG through EFI (Enzyme Function Initiative)-EST (Enzyme Similarity Tool) followed by EFI-GNT (Genome Neighborhood Tool) corroborate this highly specific pairing (Figure 2C, Table S6). As plausible explanation for the specificity of CYP redox partners,<sup>[15]</sup> is that redox proteins have co-evolved with heme-binding domain proteins such as CYPs.<sup>[16]</sup> Although the *pgn* gene cluster of *P. protegens* Pf-5 harbors a rubredoxin gene (*pngI*), the co-expression of *cayG* does not produce **1**, likely because of redox partner specificity (Figure 2B, trace b). It is conceivable that the original redox partner of CayG was CayK, but during evolution, CayG was adapted to use rubredoxin as a redox partner.

To confirm that CayG catalyzes allylic alcohol formation and to gain insight into the reaction mechanism, we next aimed at reconstituting the biotransformation *in vitro*. Soluble *N*-His<sub>6</sub>-tagged CayG and *N*-His<sub>6</sub>-tagged CayL were heterologously produced in *Escherichia coli* BL21 (DE3) (Figure S5). CayK was only obtained in soluble form as *N*-MalE-tagged. Although we tested *N*-MalE-CayK as a redox partner of CayG under several conditions (Figure S5, Table S7), no biotransformation could be observed, indicating that CayK could either not be functionally reconstituted *in vitro* or that additional factors are missing. However, we succeeded in the *in vitro* reconstitution of the CYP/rubredoxin pair. In Tris buffer with NADPH, *E. coli* flavodoxin reductase (FDR), glucose-6-phosphate, and baker's yeast glucose-6-phosphate dehydrogenase, CayG and CayL transform **2** into **1**. Interestingly, HPLC profiling of the reaction mixture and comparisons of retention times in HPLC, UV spectra, and mass spectra indicated that in addition to **1**, two other compounds (**3** and **4**) are formed (Figure 3A, trace a). When using CayG alone, we detected small amounts of **3** in addition to unreacted substrate (**2**)

(Figure 3A, trace b). Notably, the assay with CayL alone did not yield any additional product (Figure 3A, trace c).

The occurrence of these congeners in the *in vitro* biotransformations could shed light on the reaction mechanism. The UV spectrum of **3** is very similar to the one of **1**, suggesting that these metabolites share the conjugated diene-tetrayne system (Figure 3B, traces a and c). From HRMS data we deduced the molecular formula of C<sub>18</sub>H<sub>16</sub>O<sub>2</sub> ([*M*–H]<sup>–</sup> calc. 263.1078, obs. 263.1076) for **3**, which indicates that two hydrogens were abstracted from **2**. For further characterization of the highly instable **3**, we modified the terminal alkyne by Cu<sup>I</sup>-catalyzed azide-alkyne cycloaddition (CuAAC) with benzyl azide, ascorbic acid and copper (II) sulfate, and methylated the carboxy group with trimethylsilyldiazomethane (Figure S6). From the <sup>1</sup>H and <sup>1</sup>H-<sup>1</sup>H COSY spectral analysis of the stabilized derivative **5** we concluded that **3** has one additional double bond (C7–C8) (Figure S6 and Table S8). The presence of three stereoisomers (*7E/9E*, *7E/9Z*, *7Z/9E*) was detectable in the NMR spectra. Taken together, **3** represents the deoxy derivative of **1**, named deoxycaryoyncin.

The second side product of the CayG/CayL-mediated reaction (**4**, Figure 3A, trace a) has a UV spectrum similar to that of **2**, suggesting that both compounds have an enetetrayne backbone. From HRMS data of compound **4** we deduced a molecular formula of C<sub>18</sub>H<sub>17</sub>O<sub>3</sub> ([*M*–H]<sup>–</sup> calc. 281.1183, obs. 281.1183), which indicated the presence of an additional hydroxy group compared to **2**. Again, CuAAC yielded a derivative (**6**) that could be examined by NMR (Figure S7–S12). <sup>1</sup>H NMR spectral analysis supports the proposed structure of **4** as a C8-hydroxy derivative of **2**, named 8-hydroxyprotegenin. The absolute configuration (*8S*) of the secondary alcohol was determined by the Mosher method (Figure S13–S16) and proved to be identical with the secondary alcohol in **1**. Notably, we also detected traces of compound **4** in the extract of the *T. caryophylli* wild-type culture (Figure 2A, trace a).

The occurrence of **3** and **4** in the *in vitro* biotransformation assay raised the question whether these compounds are intermediates or shunt products of the CYP-mediated reaction. To clarify this, we monitored the course of the reaction by HPLC-DAD ( $\lambda=220\text{--}400\text{ nm}$ ) at selected time intervals (Figure 3C). While the size of peak for compound **1** increased at the expense of the substrate (**2**) in the course of 120 min, the peak corresponding to compound **3** grew concomitantly but reached its maximum at 60 min, then decreased and was almost gone when the reaction was stopped. Small amounts of compound **4**, on the other hand, accumulated over the course of the reaction, suggesting that the alcohol is a shunt product. To corroborate this, we subjected compound **4** to the *in vitro* assay with CayL-CayG. As predicted, **4** was not accepted as substrate for further oxidations (Figure 4C, trace b). Unexpectedly, however, purified **3**, which was first isolated from the reaction mixture and then re-subjected to a fresh CayG-CayL enzyme assay, was not transformed (Figure 4C, trace a). A plausible explanation for this observation is that the intermediate likely does not leave the enzyme cavity during

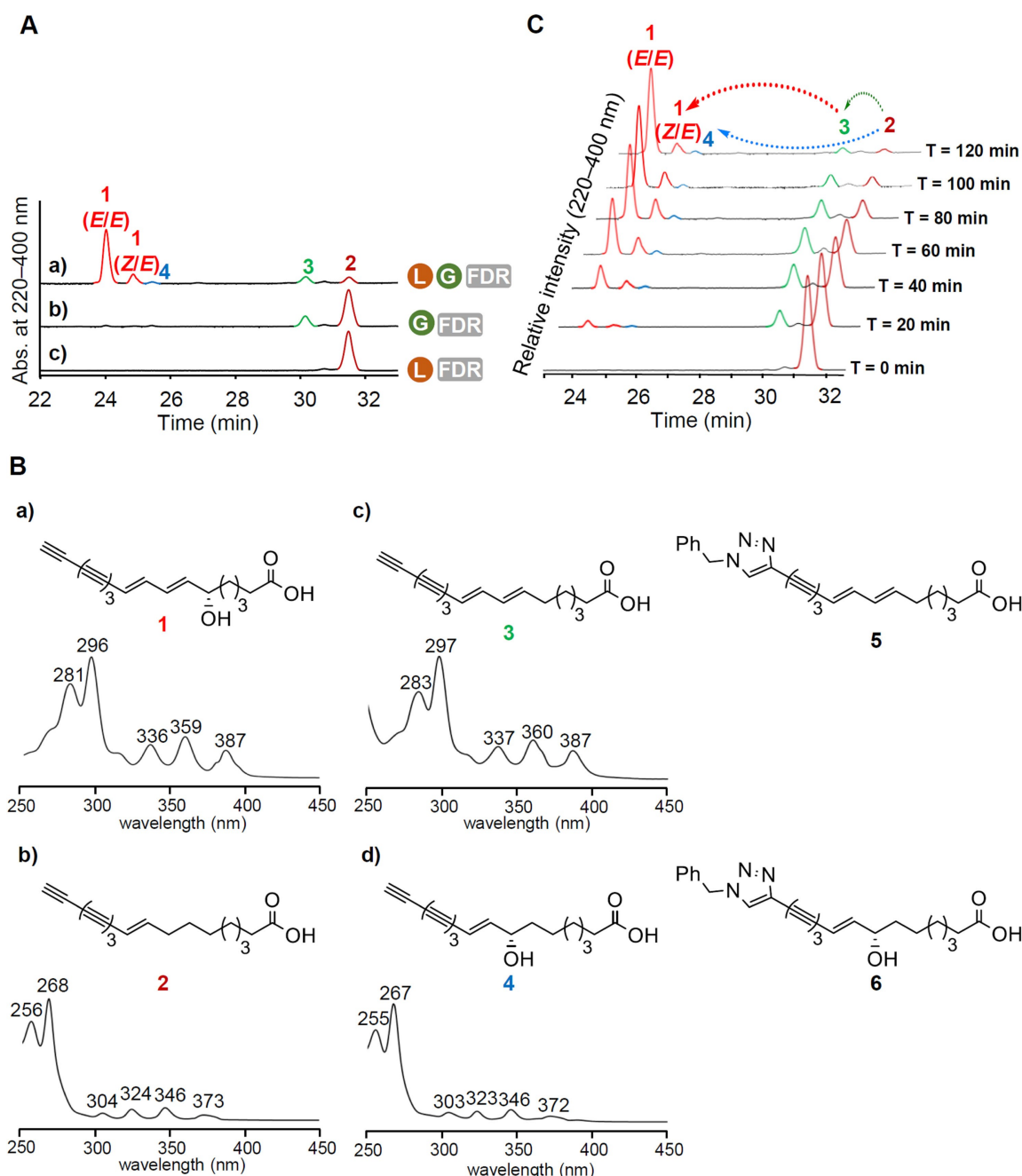


**Figure 3.** In vitro reconstitution and time course of allylic alcohol formation. A) HPLC-DAD profiles from enzyme assay with a) *N*-His<sub>6</sub> CayG and *N*-His<sub>6</sub> CayL, b) *N*-His<sub>6</sub> CayG, and c) *N*-His<sub>6</sub> CayL using FDR. B) UV spectra and chemical structures of a) protegencin (1), b) caryoynencin (2), c) intermediate 3, d) shunt product 4, and structures of stabilized derivatives 5 and 6. C) HPLC-DAD profiles of time course experiments monitoring the biotransformation of 1 into 2.

the two-step reaction, which obviously requires a conformational change of the enzyme.

To obtain potential alternative substrates for CayG, we revisited the metabolic profile of *P. protegens* and detected various protegencin congeners (7–11) with polyene fingerprint UV spectra (Figure 4A, Figure S17). HPLC-DAD-HRESI-MS analyses of these compounds revealed their molecular composition; C<sub>14</sub>H<sub>10</sub>O<sub>2</sub> for 7, C<sub>16</sub>H<sub>14</sub>O<sub>2</sub> for 8, C<sub>18</sub>H<sub>16</sub>O<sub>2</sub> for 9, C<sub>18</sub>H<sub>18</sub>O<sub>3</sub> for 10, and C<sub>18</sub>H<sub>22</sub>O<sub>3</sub> for 11. Peak

shifts in the HPLC traces after CuAAC of these compounds indicated that 7–10, but not 11, have a terminal alkyne moiety (Figure S17). Through purification and NMR analysis, we were able to elucidate the structures of these compounds (Figure 4 and Figure S18–S38). Protegencin B (7) and C (8) share the highly unstable conjugated enetetrayne structure with 2 (C18 chain) but have shorter carbon backbones (C14 and C16 chains). Protegencin D (9) and E (10) have the C18 enetetrayne framework as 2 but feature

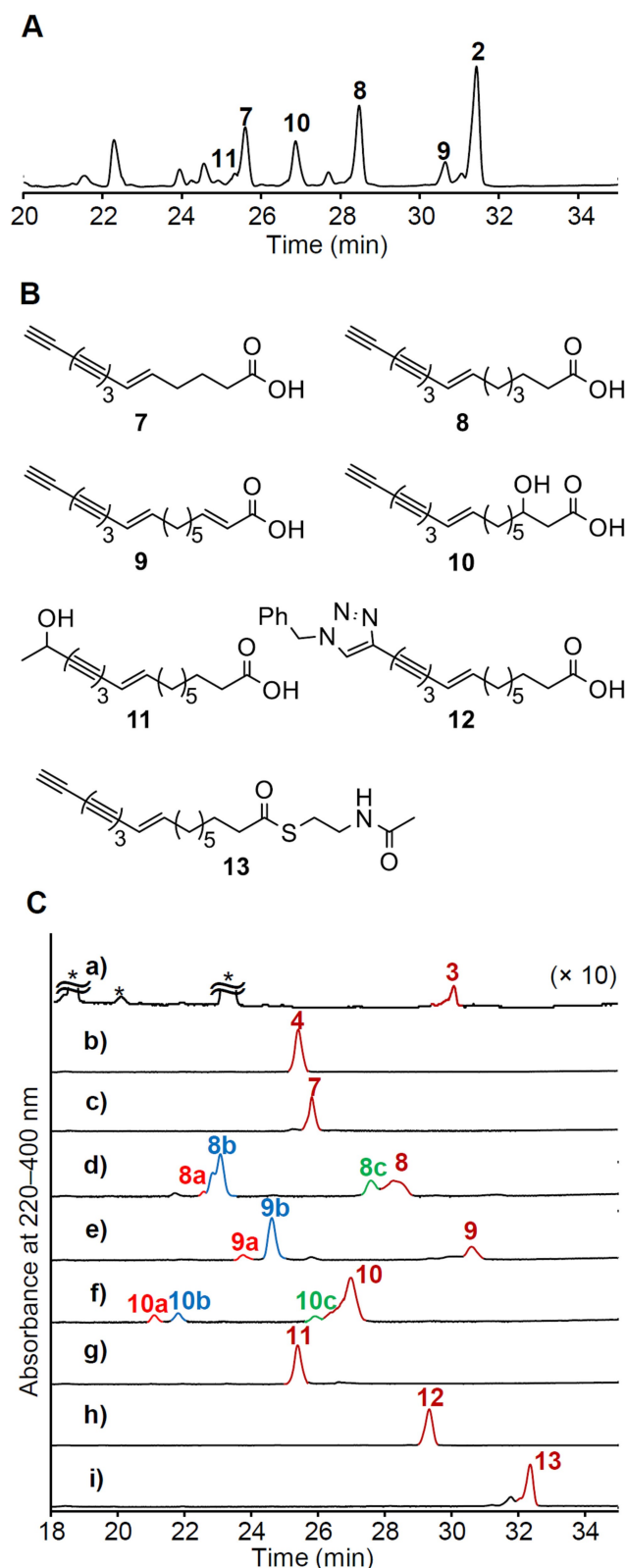


**Figure 4.** Identification of protegencin congeners B–F, and in vitro biotransformation assays using substrate analogues. A) HPLC-DAD profiles of ethyl acetate extracts obtained from incubation of *P. protegens* in TAP medium at 30 °C for 4 days. B) Chemical structures of protegencins B–F (7–11) and synthetic derivatives (12, 13). C) HPLC-DAD profiles of the in vitro biotransformation assays. Asterisks indicate non-polyyne compounds.

an additional  $\alpha,\beta$ -unsaturation or a  $\beta$ -hydroxy group, respectively. It appears that these compounds result from fatty acid  $\beta$ -oxidation. Protegenin F (11) has a secondary alcohol in lieu of the terminal alkyne and may be regarded as a shunt product of the multiple chain desaturations.<sup>[4]</sup> We also synthesized the CuAAC (12)<sup>[9b]</sup> and the phosphopantetheinyl-mimicking *N*-acetyl-cysteamine thioester (SNAC)<sup>[17]</sup> (13) derivatives of 2 (Figure S39–S43) to probe the substrate requirements of CayG.

The seven polyynes were subjected to the in vitro CayG assay, and the metabolite patterns were evaluated on the basis of retention times, UV spectra and HR-MS data. We found that CayG does not catalyze any oxygenation of the lower C14 homologue 7 (Figure 4C, trace c), whereas the C16 homologue is transformed into three new compounds that correspond to the desaturated intermediate (8c), the hydroxylated shunt product (8b), and the allylic alcohol (8a) (Figure 4C, trace d, Figure S44). Similar results were obtained using the  $\beta$ -hydroxy and  $\alpha,\beta$ -unsaturated protegencin derivatives, in all cases yielding the hydroxylated variant as the main product (Figure 4C, trace e and f, Figure S45, S46). Interestingly, triyne compounds lacking polar and/or bulky groups in place of the terminal alkyne, such as 11 and 12, are not accepted as substrates (Figure 4C, trace g and h). Likewise, conversion of the thioester 13 was not observed (Figure 4C, trace i). Thus, one may conclude that a free carboxy acid is required for the processing of the polyne backbone, but not on ACP (since the SNAC derivative mimics an ACP-bound substrate), indicating that the installation of the allylic alcohol moiety takes place after the polyne fatty acid has been liberated from the acyl carrier protein.

The results obtained from the in vitro analyses and the time-course experiments provide first insight into the reaction mechanism and the placement in the biosynthetic pathway. From the mutational analyses and the biotransformation experiments, it is evident that the installation of the allylic alcohol constitutes the final biotransformation in caryophyllene biosynthesis, after the ACP-bound polyne fatty acid has been formed by the desaturases and liberated by the thioesterase. Since CayG generates a desaturated intermediate (3) as well as a hydroxylated shunt product (4), it is likely that the reaction sequence is initiated by the enzyme-mediated abstraction of a hydrogen atom at the allylic position (C-8). The resulting allylic radical would allow entry into two alternative reaction channels, either the desaturation pathway (with sequential hydrogen abstraction at C-7) or hydroxylation. We may rule out the possibility of a hydroxylation-elimination sequence to yield a double bond, since alcohol 4 is not further transformed in the CayL-CayG enzyme assay (Figure 4C, trace b). Furthermore, we exclusively observed the direct formation of 3 in the enzyme assay with CayG. After the desaturation, CayG would hydroxylate the newly formed allylic position at C-6 of the dienetetrayne. In this transition, CayG may change its conformation to (re)position the allylic carbon atom to facilitate its hydroxylation (Figure 4C, trace a).

Competing desaturation and hydroxylation reactions have been reported for various CYPs, for example, in *trans*-

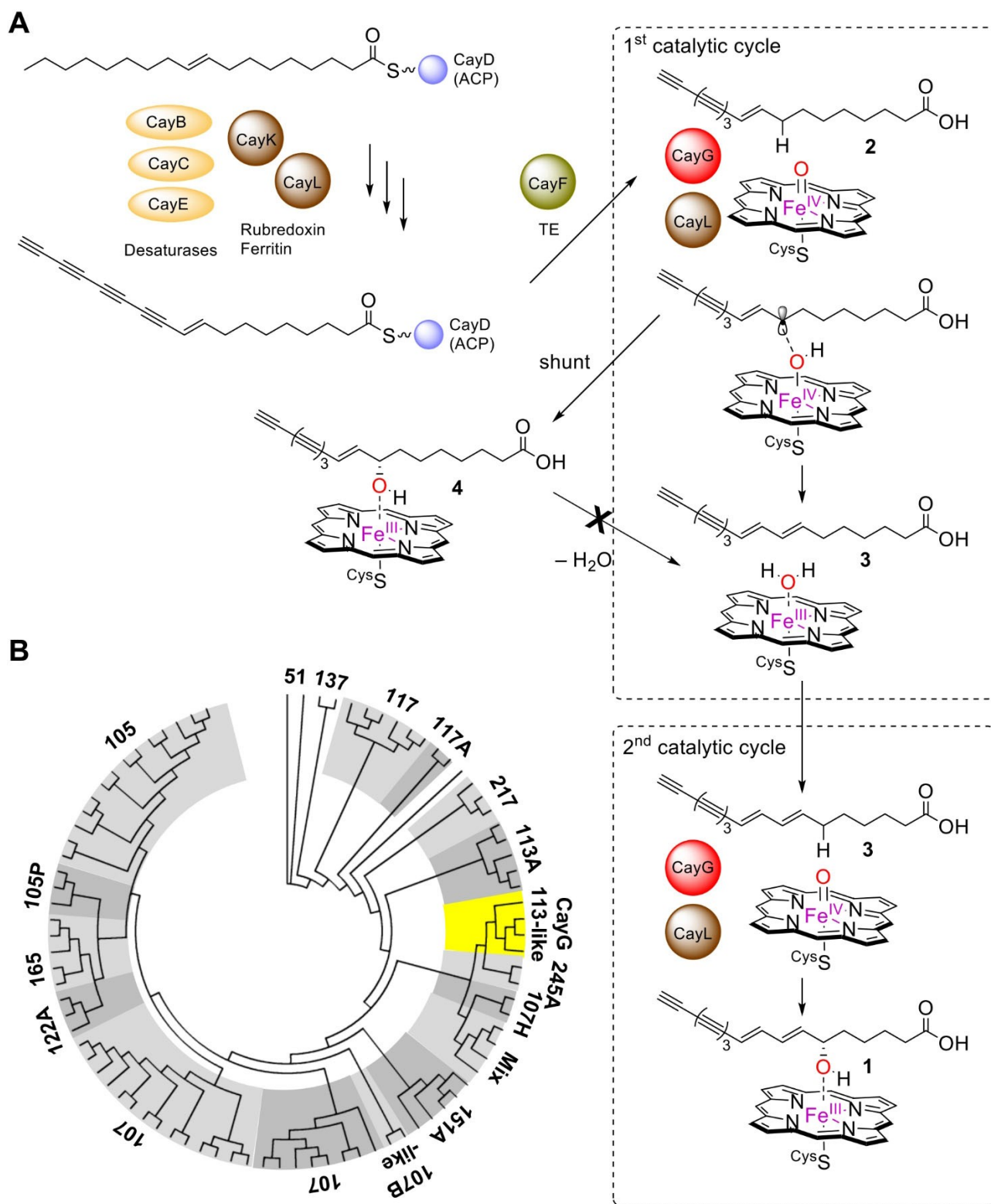


**Figure 5.** A) Model of caryoynencin biosynthesis with focus on sequential allylic alcohol formation. B) Maximum likelihood phylogenetic tree of CayG and other bacterial CYP proteins. The numbers indicate CYP clans. CayG orthologues are highlighted in yellow. Gray scales are used for separation of clans.

retinol processing of human cytochrome P450 27C1<sup>[18]</sup> and in bacterial lactimidomycin biosynthesis.<sup>[19]</sup> However, in these cases hydroxylations occurred at both adjacent carbons,

clearly reflecting lower precision than in the regio- and stereoselective allylic alcohol formation observed for CayG. In this context it is also interesting to note the unusual

pathway to allylic alcohol formation and desaturation in lovastatin biosynthesis. The fungal cytochrome P450 monooxygenase LovA catalyzes two oxidation reactions involving a tentative allylic alcohol intermediate, dehydration and double-bond shifts to give a diene, followed by a regio-divergent hydroxylation of the decalin core.<sup>[20]</sup> On the basis of our findings and the different structural prerequisites in both systems, CayG catalysis clearly differs from previously described mechanisms.

To evaluate the distinctiveness of CayG, we generated a maximum likelihood phylogenetic tree (Figure 5B, Figure S47, and Table S9). The phylogenetic analysis shows that CayG forms an own clade of CYP113-like protein. A remarkable feature of CayG is the use of both a rubredoxin and a ferritin-like protein as designated redox partner. In our knowledge, these proteins which contain iron(s), but not possess inorganic sulfide, have not yet been reported as electron donors for CYPs.<sup>[21]</sup> Only recently, it was shown that viability- and virulence-related CYP from *Mycobacterium tuberculosis* could use rubredoxin instead of ferredoxin under iron-deficient conditions.<sup>[22]</sup> However, both CYP-rubredoxin and -ferritin-like protein systems are unprecedented in the context of specialized biosynthetic pathways.

## Conclusion

In conclusion, we demonstrated that sequential olefination and hydroxylation on protegencin (**2**) in the biosynthetic pathway of caryophenol (**1**) is accomplished by a single multifunctional cytochrome P450 monooxygenase CayG. CayG is the first example for a CYP to catalyze allylic alcohol formation from a saturated carbon chain and thus represents an important addition to the family of multifunctional oxygenases. It was noteworthy that both CayK and CayL are rare designated CYP redox partners. Interestingly, the CayG-mediated desaturation and hydroxylation reactions may be dissected depending on the reducing system and the substrates employed. The results from the biotransformation experiments using protegencin homologues and derivatives indicate that this sequential process promoted by CayG is highly coordinated as it may be derailed or even abolished when the carbon chain does not match the preferred size of the substrate. Furthermore, both the carboxy and the alkyne termini are important for substrate recognition and docking to the active site. These results expand our current understanding of cytochrome P450 monooxygenase and may be helpful to develop new multifunctional (bio)catalysts for the regio- and stereoselective modification of saturated carbon backbones.

## Acknowledgements

We thank A. Perner for LC HR-MS measurements, H. Heinecke for NMR measurements, E. Herzog and F. Guide for MALDI-TOF measurements. Financial support by the Deutsche Forschungsgemeinschaft (DFG, German Research Foundation) "Project-ID 239748522" SFB 1127, and Leibniz

Award (to C.H.), and the PAKT für Forschung und Innovation is gratefully acknowledged. Open Access funding enabled and organized by Projekt DEAL.

## Conflict of Interest

The authors declare no conflict of interest.

## Data Availability Statement

The data that support the findings of this study are available in the Supporting Information of this article.

**Keywords:** Alkynes · Biosynthesis · Fatty Acids · Natural Products · Oxygenase

- [1] a) F. P. Guengerich in *In Cytochrome P450: Structure, Mechanism, and Biochemistry*, 4th ed. (Ed.: P. R. Ortiz de Montellano), Springer International Publishing, Cham, **2015**, pp. 523–785; b) L. M. Podust, D. H. Sherman, *Nat. Prod. Rep.* **2012**, *29*, 1251–1266.
- [2] J. D. Rudolf, C.-Y. Chang, M. Ma, B. Shen, *Nat. Prod. Rep.* **2017**, *34*, 1141–1172.
- [3] R. V. K. Cochrane, J. C. Vederas, *Acc. Chem. Res.* **2014**, *47*, 3148–3161.
- [4] C. Ross, K. Scherlach, F. Kloss, C. Hertweck, *Angew. Chem. Int. Ed.* **2014**, *53*, 7794–7798; *Angew. Chem.* **2014**, *126*, 7928–7932.
- [5] T. Kusumi, I. Ohtani, K. Nishiyama, H. Kakisawa, *Tetrahedron Lett.* **1987**, *28*, 3981–3984.
- [6] B. Dose, T. Thongkongkaew, D. Zopf, H. J. Kim, E. V. Bratovanov, M. G. Pérez, K. Scherlach, J. Krabbe, C. Ross, R. Hermentau, S. P. Niehs, A. Silge, J. Hniopek, M. Schmitt, J. Popp, C. Hertweck, *ChemBioChem* **2021**, *22*, 2901–2907.
- [7] L. V. Flórez, K. Scherlach, P. Gaube, C. Ross, E. Sitte, C. Hermes, A. Rodrigues, C. Hertweck, M. Kaltenpoth, *Nat. Commun.* **2017**, *8*, 15172.
- [8] M. Yamaguchi, H.-J. Pakr, S. Ishizuka, K. Omata, M. Hiramata, *J. Med. Chem.* **1995**, *38*, 5015–5022.
- [9] a) A. J. Mullins, G. Webster, H. J. Kim, J. Zhao, Y. D. Petrova, C. E. Ramming, M. Jenner, J. A. H. Murray, T. R. Connor, C. Hertweck, G. L. Challis, E. Mahenthiralingam, *mBio* **2021**, *12*, e0071521; b) V. Hotter, D. Zopf, H. J. Kim, A. Silge, M. Schmitt, P. Aiyar, J. Fleck, C. Matthaus, J. Hniopek, Q. Yan, J. Loper, S. Sasso, C. Hertweck, J. Popp, M. Mittag, *Proc. Natl. Acad. Sci. USA* **2021**, *118*, e2107695118; c) K. Murata, M. Suenaga, K. Kai, *ACS Chem. Biol.* **2021**, <https://doi.org/10.1021/acscchembio.1c00276>.
- [10] J. M. Blatny, T. Brautaset, H. C. Winther-Larsen, P. Karunakaran, S. Valla, *Plasmid* **1997**, *38*, 35–51.
- [11] S. C. Andrews, *Biochim. Biophys. Acta Gen. Subj.* **2010**, *1800*, 691–705.
- [12] Y. Nie, J. Liang, H. Fang, Y. Q. Tang, X. L. Wu, *Appl. Environ. Microbiol.* **2011**, *77*, 7279–7288.
- [13] a) A. J. Mullins, J. A. H. Murray, M. J. Bull, M. Jenner, C. Jones, G. Webster, A. E. Green, D. R. Neill, T. R. Connor, J. Parkhill, G. L. Challis, E. Mahenthiralingam, *Nat. Microbiol.* **2019**, *4*, 996–1005; b) K. Kai, M. Sogame, F. Sakurai, N. Nasu, M. Fujita, *Org. Lett.* **2018**, *20*, 3536–3540.
- [14] a) J. A. Gerlt, J. T. Bouvier, D. B. Davidson, H. J. Imker, B. Sadkhin, D. R. Slater, K. L. Whalen, *Biochim. Biophys. Acta*

- Proteins Proteomics* **2015**, *1854*, 1019–1037; b) R. Zallot, N. Oberg, J. A. Gerlt, *Biochemistry* **2019**, *58*, 4169–4182.
- [15] T. Zhang, L. Du, F. Li, X. Zhang, Z. Qu, L. Han, Z. Li, J. Sun, F. Qi, Q. Yao, Y. Sun, C. Geng, S. Li, *ACS Catal.* **2018**, *8*, 9992–10003.
- [16] A. Harel, Y. Bromberg, P. G. Falkowski, D. Bhattacharya, *Proc. Natl. Acad. Sci. USA* **2014**, *111*, 7042–7047.
- [17] J. Franke, C. Hertweck, *Cell Chem. Biol.* **2016**, *23*, 1179–1192.
- [18] K. M. Johnson, T. T. N. Phan, M. E. Albertolle, F. P. Guengerich, *J. Biol. Chem.* **2017**, *292*, 13672–13687.
- [19] J.-W. Seo, M. Ma, T. Kwong, J. Ju, S.-K. Lim, H. Jiang, J. R. Lohman, C. Yang, J. Cleveland, E. Zazopoulos, C. M. Farnet, B. Shen, *Biochemistry* **2014**, *53*, 7854–7865.
- [20] J. Barriuso, D. T. Nguyen, J. W.-H. Li, J. N. Roberts, G. MacNevin, J. L. Chaytor, S. L. Marcus, J. C. Vederas, D.-K. Ro, *J. Am. Chem. Soc.* **2011**, *133*, 8078–8081.
- [21] S. Li, L. Du, R. Bernhardt, *Trends Microbiol.* **2020**, *28*, 445–454.
- [22] T. Sushko, A. Kavaleuski, I. Grabovec, A. Kavaleuskaya, D. Vakhrameev, S. Bukhdruker, E. Marin, A. Kuzikov, R. Masamrekh, V. Shumyantseva, K. Tsumoto, V. Borshchevskiy, A. Gilep, N. Strushkevich, *Bioorg. Chem.* **2021**, *109*, 104721.

Manuscript received: March 2, 2022

Accepted manuscript online: April 13, 2022

Version of record online: April 29, 2022